

Experimental Results from Heavy Ion Collisions at LHC

Ranbir Singh¹, Lokesh Kumar², Pawan Kumar Netrakanti³ and Bedangadas Mohanty⁴

¹*Physics Department, University of Jammu, Jammu 180001, India,*

²*Kent State University, Kent, Ohio 44242, USA,*

³*Nuclear Physics Division, Bhabha Atomic Research Centre, Mumbai 400 085, India, and*

⁴*School of Physical Sciences, National Institute of Science Education and Research, Bhubaneswar 751005, India*

(Dated: February 9, 2019)

We review a subset of experimental results from the heavy-ion collisions at the Large Hadron Collider (LHC) facility at CERN. Excellent consistency is observed for various measurements like charged particle multiplicity density, second order azimuthal anisotropy and nuclear modification factor of charged hadrons across all the experiments at the LHC. Comparison to corresponding results from the collisions at lower energy (centre of mass energy, $\sqrt{s_{NN}} = 200$ GeV) at the Relativistic Heavy Ion Collider (RHIC) facility shows that system formed at LHC ($\sqrt{s_{NN}} = 2.76$ TeV) produces a larger number of particles per participating nucleon pair, attains higher energy density, has a larger system size, and lives for a longer time. Higher collision energy at LHC allows measurements to uncover interesting observations at kinematic regions in pseudorapidity and transverse momentum not previously measured in the heavy-ion collisions. Finally, we compare the LHC measurements to some model calculations to get a glimpse of the physical insight provided by these measurements.

PACS numbers: 25.75.-q, 25.75.Ag, 25.75.Bh

I. INTRODUCTION

The main goal of the high energy heavy-ion collisions is to study the phase structure of the Quantum Chromodynamic (QCD) phase diagram[1–3]. One of the most interesting aspects of these collisions is the possibility of forming a phase of de-confined quarks and gluons, a system that is believed to have existed in a few microsecond old Universe. First principle QCD calculations suggest that it is possible to have such a state of matter if the temperatures attained can be of the order of the QCD scale (~ 200 MeV) [4–6]. In laboratory, such temperatures could be attained by colliding heavy-ions at relativistic energies. Further, at very high energies as encountered for heavy-ion collisions at LHC and RHIC, the de-confined phase could stay for long enough durations enabling to study the properties of the fundamental constituent (quarks and gluons) of any visible matter.

The results from heavy-ion collisions at RHIC have clearly demonstrated the formation of a de-confined system of quarks and gluons in Au+Au collisions at $\sqrt{s_{NN}} = 200$ GeV [7–11]. The produced system exhibits copious production of strange hadrons, shows substantial collectivity developed in the partonic phase, exhibits suppression in high transverse momentum (p_T) hadron production relative to $p+p$ collisions and small fluidity as reflected by a small value of viscosity to entropy density ratio (η/s). A factor of about 14 increase in energy for Pb+Pb collisions at LHC is expected to unravel the temperature dependence of various observables as well to provide an extended kinematic region in rapidity and p_T where measurements in heavy-ion col-

lisions did not exist previously. On the other hand, at RHIC a beam energy scan program is being undertaken to explore the other details of the QCD phase diagram [12].

In this review paper, we discuss a subset of results that have come out from LHC Pb+Pb collisions at $\sqrt{s_{NN}} = 2.76$ TeV. We have divided the discussion into three sections. In the second section we discuss the consistency of various measurements among the three LHC experiments that have heavy-ion programs: ALICE, CMS and ATLAS. In the third section, we make a comparative study between similar observables measured at lower energy collisions at RHIC to those from LHC. In doing this, we highlight the additional information that heavy-ion collisions at LHC bring compared to RHIC. In the fourth section, we present a comparison of various model calculations to the corresponding measurements at LHC. Finally we summarize our observations in the last section of the article.

II. CONSISTENCY OF RESULTS AMONG LHC EXPERIMENTS

A. Charged particle multiplicity

One of the first measurements to come out of the heavy-ion collision program at LHC is the charged particle multiplicity per unit pseudorapidity in Pb+Pb collisions at $\sqrt{s_{NN}} = 2.76$ TeV. Figure 1 shows the centrality (reflected by the number of participating nucleons, N_{part} , obtained from a Glauber model calculation [13]) dependence of $dN_{ch}/d\eta$ at midrapidity for Pb+Pb collisions at $\sqrt{s_{NN}} = 2.76$

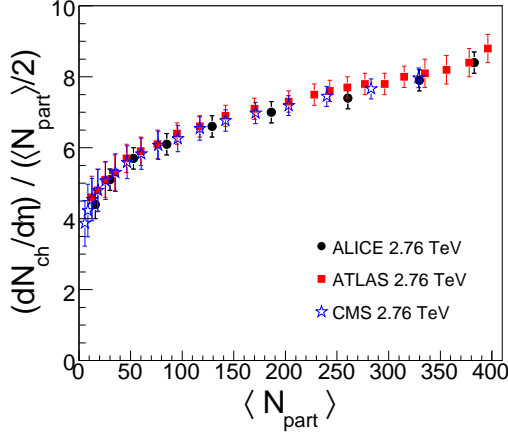


FIG. 1: (Color online) Average charged particle multiplicity density per unit pseudorapidity ($dN_{\text{ch}}/d\eta$) at midrapidity per participating nucleon (N_{part}) pair plotted as a function of N_{part} for Pb+Pb collisions at $\sqrt{s_{\text{NN}}} = 2.76$ TeV. The measurements are shown from ALICE [14], CMS [15] and ATLAS [16] experiments.

TeV from ALICE [14], CMS [15] and ATLAS [16] experiments. The error bars reflect statistical uncertainties.

The ATLAS measurements of $dN_{\text{ch}}/d\eta|_{\eta=0}$ are obtained over $|\eta| < 0.5$ using a minimum bias trigger with a central solenoid magnet off data set. The

charged particles are reconstructed using two different algorithms using the information from pixel detectors covering $|\eta| < 2.0$. The N_{part} values are obtained by comparing the summed transverse energy in the forward calorimeter over a pseudorapidity range $3.2 < |\eta| < 4.9$ to a Glauber model simulation. The CMS results $dN_{\text{ch}}/d\eta|_{\eta=0}$ are from the barrel section of the pixel tracker covering $|\eta| < 2.5$. The minimum bias trigger data set was in the magnetic field off configuration so as to improve the acceptance of low p_T particles. The centrality determination as in the case of ATLAS experiment are done using information from hadron forward calorimeter ($2.9 < |\eta| < 5.2$) and Glauber model simulations. The ALICE measurement uses a minimum bias data set from the silicon pixel detector ($|\eta| < 2.0$). The centrality selection is carried out using signals from VZERO detectors (2 arrays of 32 scintillators tiles) covering the region $2.8 < \eta < 5.1$ and $-3.7 < \eta < -1.7$, along with the corresponding Glauber modeling of the data.

In spite of difference in operating conditions and measurement techniques, the $dN_{\text{ch}}/d\eta$ versus N_{part} results for Pb+Pb collisions at $\sqrt{s_{\text{NN}}} = 2.76$ TeV shows a remarkable consistency across the three experiments.

B. Azimuthal anisotropy

Figure 2 shows the azimuthal anisotropy of produced charged particles ($v_n = \langle \cos(n(\phi - \Psi_n)) \rangle$) as a function of p_T for 30-40% Pb+Pb collisions at $\sqrt{s_{\text{NN}}} = 2.76$ TeV. Here ϕ is the azimuthal angle of the produced particles and Ψ_n is the n^{th} order reaction plane angle measured in the experiments.

In the CMS experiment [17] the v_2 measurements use the information from the silicon tracker in the region $|\eta| < 2.5$ with a track momentum resolution of 1% at $p_T = 100$ GeV/c and kept within a magnetic field of 3.8 Tesla. The event plane angle (Ψ_2) is obtained using the information on the energy deposited in the hadron forward calorimeter. A minimum η gap of 3 units is kept between the particles used for obtaining Ψ_2 and v_2 . This ensures suppression of non-flow correlations which could arise for example from dijets. The event plane resolution obtained using three sub event technique varies from 0.55 to 0.84, depending on the collision centrality. The ATLAS experiment [18] measured v_n using the inner detectors in the $|\eta| < 2.5$, kept inside a 2 Tesla field of superconducting solenoid magnet. The event planes are obtained using forward calorimeter information, with resolution varying from 0.2 to 0.85 depending on collision centrality. The ALICE experiment [19] measured v_n using charged tracks reconstructed from the Time Projection Chamber ($|\eta| < 0.8$), the event plane was obtained using information from VZERO detectors kept at a large rapidity gap from the TPC. The momentum resolution of the tracks are better than 5%.

A very nice agreement for v_2 , v_3 and v_4 values versus p_T to a level of within 10% for most of the p_T range presented is found between all the experiments.

C. Nuclear modification factor

Figure 3 shows the nuclear modification factor for inclusive charged hadrons measured at midrapidity in LHC experiments for Pb+Pb collisions at $\sqrt{s_{\text{NN}}} = 2.76$ TeV. The nuclear modification factor is de-

fined as $R_{AA} = \frac{dN_{AA}/d\eta d^2p_T}{T_{AB} d\sigma_{NN}/d\eta d^2p_T}$, here the overlap integral $T_{AB} = N_{\text{binary}}/\sigma_{\text{inelastic}}^{pp}$ with N_{binary} being the number of binary collisions commonly estimated from Glauber model calculation and $d\sigma_{NN}/d\eta d^2p_T$ is the cross section of charged hadron production in $p+p$ collisions at $\sqrt{s} = 2.76$ TeV. The result shows

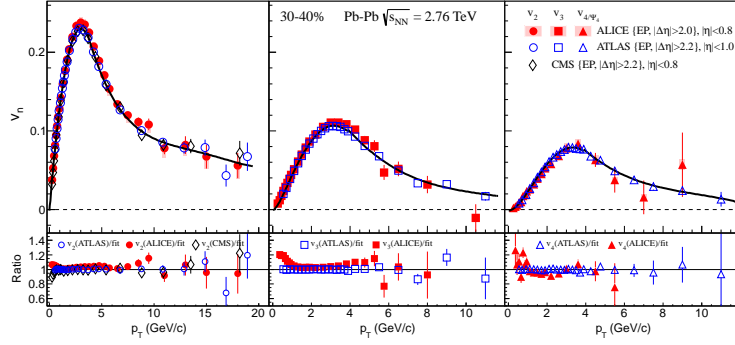


FIG. 2: (Color online) v_n versus p_T at midrapidity for 30-40% Pb+Pb collisions at $\sqrt{s_{NN}} = 2.76$ TeV. The results are shown from different LHC experiments: CMS [17], ATLAS [18] and ALICE [19]. The bottom panels shows the ratio of the experimental data to a polynomial fit to the ALICE data.

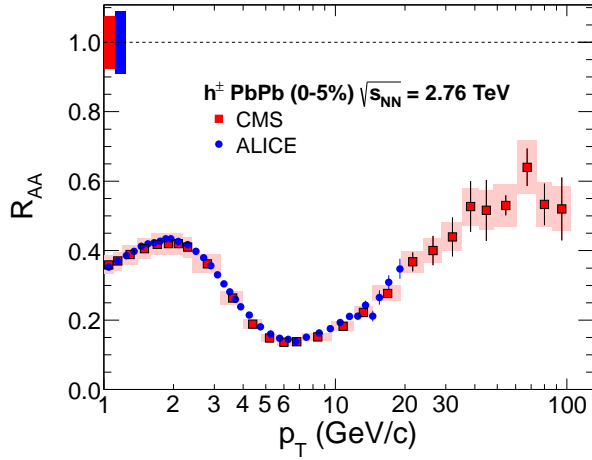


FIG. 3: (Color online) Nuclear modification factor R_{AA} of charged hadrons measured by ALICE [20] and CMS [21] experiments at midrapidity for 0-5% most central Pb-Pb collisions at $\sqrt{s_{NN}} = 2.76$ TeV. The boxes around the data denote p_T -dependent systematic uncertainties. The systematic uncertainties on the normalization are shown as boxes at $R_{AA} = 1$.

that the charged particle production at high p_T in LHC is suppressed in heavy-ion collisions relative to nucleon-nucleon collisions.

The ALICE experiment [20] uses the Inner Tracking System (ITS) and the Time Projection Chamber (TPC) for vertex finding and tracking in a minimum bias data set. The CMS experiment [21] reconstructs charged particles based on hits in the silicon pixel and strip detectors. In order to extend the statistical reach of the p_T spectra in the highly pre-scaled minimum bias data recorded in 2011 it uses unpre-scaled single-jet triggers. Both experiments take the value of $\sigma_{inelastic}^{pp} = 64 \pm 5$ mb.

An excellent agreement for R_{AA} versus p_T for charged hadrons in 0-5% central Pb+Pb collisions

at $\sqrt{s_{NN}} = 2.76$ TeV is observed between the two experiments.

Having discussed the consistency of these first measurements in Pb+Pb collisions among different experiments, the major detectors used, acceptances and ways to determine centrality and event plane, we now discuss the comparison between measurements at RHIC and LHC heavy-ion collisions.

III. COMPARISON OF LHC AND RHIC RESULTS

In the first subsection, we discuss the energy dependence of basic measurements made in heavy-ion collisions. These include $dN_{ch}/d\eta$, $\langle m_T \rangle$ ($m_T = \sqrt{p_T^2 + \text{mass}^2}$), Bjorken energy density (ϵ_{Bj}), life time of the hadronic phase (τ_f), system volume at the freeze-out, kinetic and chemical freeze-out conditions and finally the fluctuations in net-charge distributions. In the next subsection, we discuss about the energy dependence of p_T integrated v_2 which is a measure of collectivity, followed by comparisons of v_n versus p_T and flow fluctuations at RHIC and LHC. In the final subsection, we compare the nuclear modification factor for hadrons produced in heavy-ion collisions at RHIC and LHC.

A. Bulk properties at freeze-out

1. Multiplicity

Figure 4 (top panel) shows the charged particle multiplicity density at midrapidity ($dN_{ch}/d\eta$) per participating nucleon pair produced in central heavy-ion collisions versus $\sqrt{s_{NN}}$. We observe that the charged particle production increases by a factor 2 as the energy increases from RHIC to LHC.

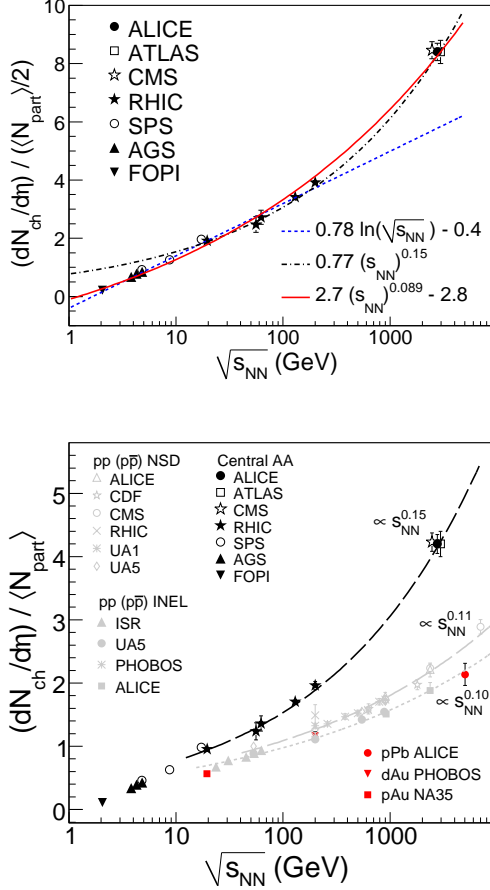


FIG. 4: (Color online) Top panel: $dN_{ch}/d\eta$ per participating nucleon pair at midrapidity in central heavy ion collisions as a function of $\sqrt{s_{NN}}$. Bottom panel: Comparison of $dN_{ch}/d\eta$ per participating nucleon at midrapidity in central heavy-ion collisions [15, 16, 22–30] to corresponding results from $p+p(\bar{p})$ [31–39] and $p(d)+A$ collisions [22, 40, 41].

The energy dependence seems to rule out a logarithmic dependence of particle production with $\sqrt{s_{NN}}$ and supports a power law type of dependence on $\sqrt{s_{NN}}$. Figure 4 (bottom panel) shows the excess of $dN_{ch}/d\eta/\langle N_{part} \rangle$ in A+A collisions [15, 16, 22–30] over corresponding yields in $p+p(\bar{p})$ [31–39] and $p(d)+A$ collisions [22, 40, 41]. This observation also seen at RHIC persists at LHC but is proportionately larger at the higher energy collisions at the LHC. A power law fit to the $p+p$ collision charged particle multiplicity density leads to a dependence $\sim s^{0.11}$, while those for A+A collisions goes as $\sim s^{0.15}$. This is a clear indication that A+A collisions at RHIC and LHC are not a simple superposition of several $p+p$ collisions, whereas the $p+A$ collisions seem to closely follow this superposition principle.

2. Average transverse mass and Bjorken energy density

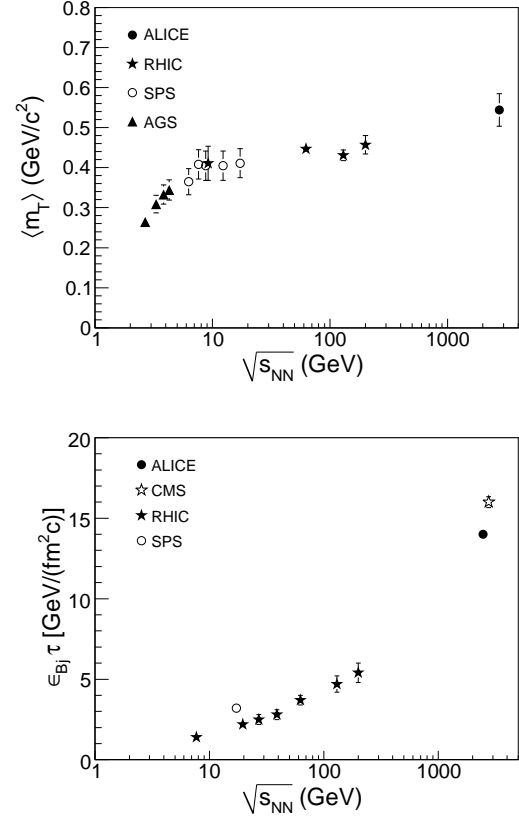


FIG. 5: (Color online) Top panel: $\langle m_T \rangle$ for charged pions in central heavy-ion collisions at midrapidity for AGS [42, 43], SPS [44, 45], RHIC [33, 46] and LHC [47] energies. The errors shown are the quadrature sum of statistical and systematic uncertainties. Bottom panel: The product of Bjorken energy density, ϵ_{Bj} [48], and the formation time (τ) in central heavy ion collisions at mid-rapidity as a function of $\sqrt{s_{NN}}$ [49–54].

Figure 5 top panel shows the $\langle m_T \rangle$ values for pions in central heavy-ion collisions as a function of $\sqrt{s_{NN}}$. The $\langle m_T \rangle$ value increases with $\sqrt{s_{NN}}$ at lower AGS energies [42, 43], stays independent of $\sqrt{s_{NN}}$ for the SPS energies [44, 45] and then tends to rise further with increasing $\sqrt{s_{NN}}$ at the higher beam energies of LHC. About 25% increase in $\langle m_T \rangle$ is observed from RHIC [33, 46] to LHC [47]. For a thermodynamic system, $\langle m_T \rangle$ can be an approximate representation of the temperature of the system, and $dN/dy \propto \ln(\sqrt{s_{NN}})$ may represent its entropy [55]. In such a scenario, the observations could reflect the characteristic signature of a phase transition, as proposed by Van Hove [56]. Then, the constant value of $\langle m_T \rangle$ vs. $\sqrt{s_{NN}}$ has one possible interpretation in terms of formation of a mixed phase of a QGP

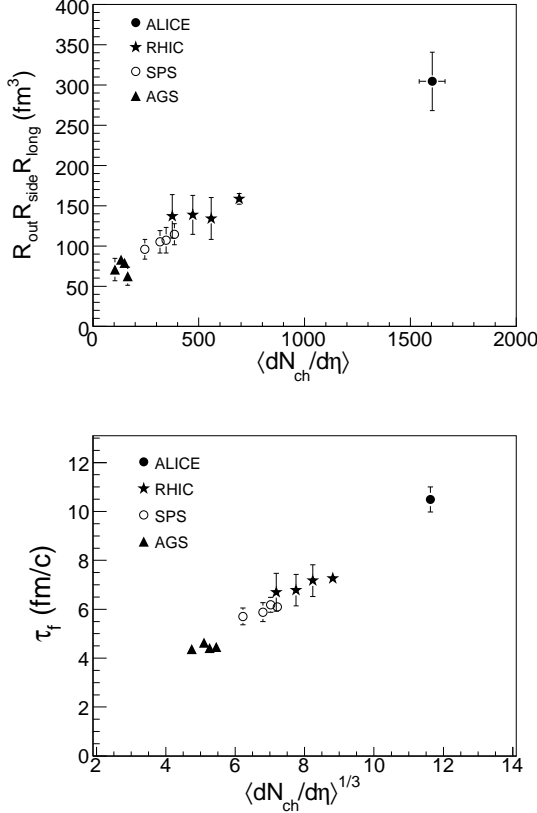


FIG. 6: (Color online) Top panel: Product of the three pion HBT radii at k_T (average transverse momenta of two pions) = 0.3 GeV/c for central heavy-ion collisions at AGS [57], SPS [58, 59], RHIC [60, 61] and LHC [62] energies. Bottom panel: The decoupling time extracted from $R_{\text{long}}(k_T)$ for central heavy-ion collisions at midrapidity at AGS, SPS, RHIC and LHC energies as a function of $(dN_{\text{ch}}/d\eta)^{1/3}$.

and hadrons during the evolution of the heavy-ion system. The energy domains accessed at RHIC and LHC will then correspond to partonic phase while those at AGS would reflect hadronic phase. However, there could be several other effects to which $\langle m_T \rangle$ is sensitive, which also need to be understood for proper interpretation of the data [55].

Figure 5 bottom panel shows the product of the estimated Bjorken energy density ($\epsilon_{Bj} = \frac{1}{A_{\perp}\tau} dE_T/dy$; A_{\perp} [48] is the transverse overlap area of the nuclei and E_T is the transverse energy) and formation time (τ) as a function of $\sqrt{s_{\text{NN}}}$ [49–54]. The energy density at LHC seems to be a factor 3 larger compared to those attained at RHIC.

3. Volume and decoupling time

The top panel of Fig. 6 shows the energy dependence of the product of the three radii (R_{out} , R_{side} and R_{long}) obtained from pion HBT analysis. Here the “out” corresponds to the axis pointing along the pair transverse momentum, the “side” to the axis perpendicular to it in the transverse plane, and the “long” axis being along the beam (Bertsch-Pratt convention [63, 64]). The product of the radii is connected to the volume of the homogeneity region at the last interaction. The product of the three radii shows a linear dependence on the charged-particle pseudorapidity density. The data indicates that the volume of homogeneity region is two times larger at the LHC than at RHIC.

Further, within a hydrodynamic picture, the decoupling time for hadrons (τ_f) at midrapidity can be estimated from the magnitude of radii R_{long} . With $R_{\text{long}}^2 = \tau_f^2 T K_2(m_T/T)/m_T K_1(m_T/T)$, with $m_T = \sqrt{m_{\pi}^2 + k_T^2}$, where m_{π} is the mass of the pion, T is the kinetic freeze-out temperature (taken as 120 MeV) and K_1 and K_2 are the integer order modified Bessel functions. The extracted τ_f values for central heavy-ion collisions at midrapidity at AGS [57], SPS [58, 59], RHIC [60, 61] and LHC [62] energies are shown as a function of cube-root of $dN_{\text{ch}}/d\eta$ in the bottom panel of Fig. 6. We observe that τ_f scales linearly with $(dN_{\text{ch}}/d\eta)^{1/3}$ and is about 10 fm/c at LHC energies. Note the value is about 40% larger than at RHIC. However there are few caveats which needs to be kept in mind, the above expression ignores transverse expansion of the system, finite chemical potential for pions and uncertainties associated with freeze-out temperature. These effects are to some extent reflected in the uncertainties shown on the data points.

4. Temperature and collective flow velocity

The hadron yields and spectra reflects the properties of the bulk matter at chemical and kinetic freeze-out, respectively. Generally, the point at which the inelastic collisions ceases is called the chemical freeze-out and the point where even the elastic collisions stop is called the kinetic freeze-out.

The transverse momentum distribution of different particles contains two components, one random and the other collective. The random component can be identified with the temperature of the system at kinetic freeze-out (T_{kin}). The collective component, which could arise from the matter density gradient from the center to the boundary of the fireball created in high energy nuclear collisions is called collective flow in transverse direction ($\langle \beta \rangle$). Using the

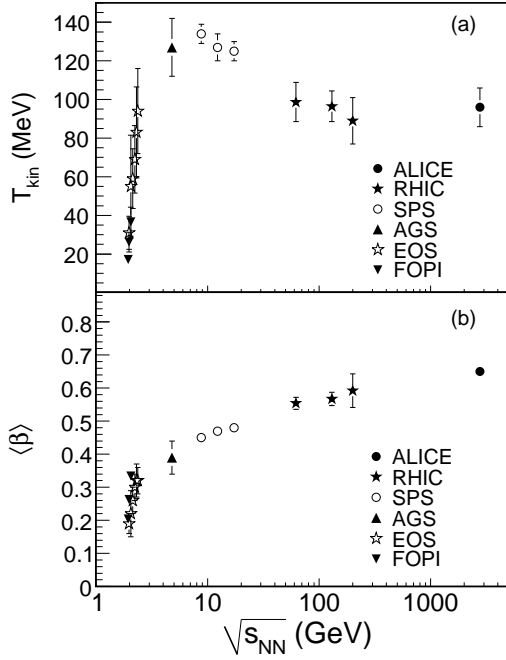


FIG. 7: (Color online) Kinetic freeze-out temperature and collective flow velocity in central heavy-ion collisions as a function of collision energy. [33, 47, 65–68]

assumption that the system attains thermal equilibrium, the blast wave formulation can be used to extract T_{kin} and $\langle\beta\rangle$. These two quantities are shown in Fig. 7 versus $\sqrt{s_{\text{NN}}}$ [33, 47, 65–68]. For beam energies at AGS and above, one observes a decrease in T_{kin} with $\sqrt{s_{\text{NN}}}$. This indicates that higher the beam energy, longer is the interactions among the constituents of the expanding system and lower the temperature. From RHIC top energy to LHC there seems to be however a saturation in the value of T_{kin} . In contrast to the temperature the collective flow increases with increase in beam energy rapidly, reaching a value close to 0.6 times the speed of light at the LHC energy.

Figure 8 shows the chemical freeze-out temperature (T_{ch}) versus the baryon chemical potential (μ_{B}) in central heavy-ion collisions [33, 47, 69–76]. These quantities are obtained by fitting the particle yields to a statistical model assuming thermal equilibrium within the framework of a Grand Canonical ensemble. There are two values of temperature quoted for LHC energies. A T_{ch} value of about 164 MeV and fixed μ_{B} value of 1 MeV seems to reproduce the multi-strange ratios (involving Ξ and Ω) quite well, but were observed to miss the data for p/π and Λ/π . On the other hand, the statistical ther-

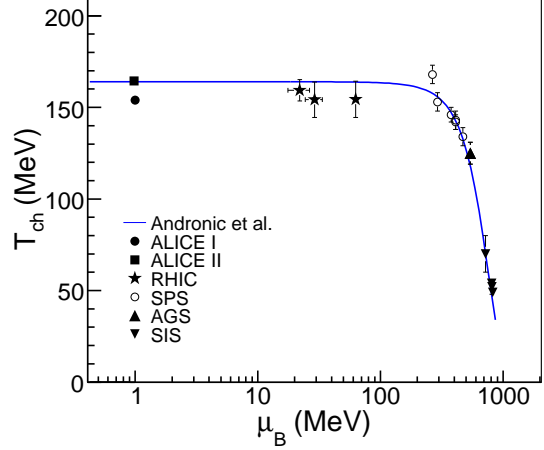


FIG. 8: (Color online) Chemical freeze-out temperature versus baryon chemical potential in central heavy-ion collisions [33, 47, 69–76]. The curve corresponds to model calculations from Ref. [69, 70].

mal model prediction with $T_{\text{ch}} = 152$ MeV and fixed $\mu_{\text{B}} = 1$ MeV fits the measured p/π and Λ/π ratios better but misses the ratios involving multi-strange hadrons [77]. This issue is not yet resolved, with being possibly related to hadronic final state interactions [78]. The curve corresponds to model calculations from Ref. [69, 70].

5. Fluctuations

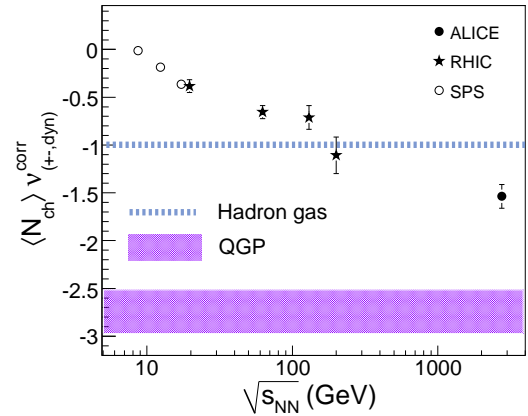


FIG. 9: (Color online) Energy dependence of net-charge fluctuations about midrapidity in central heavy-ion collisions at SPS [79], RHIC [80] and LHC [81] energies. Also shown are the expectations from a hadron resonance gas model and for a simple QGP picture [82].

The fluctuation in net-charge depends on the square of the charge state of the system. They are good indicators of phase transition, where the partonic phase have constituents with fractional charges while the hadronic phase has constituents with integral units. Hence, net-charge fluctuations are expected to be smaller if the system underwent a phase transition and freeze-out is close to the phase transition temperature so that the signals survive. An experimental measure of net-charge fluctuations is defined as $\nu(+-, dyn) = \frac{\langle N_+(N_+-1) \rangle}{\langle N_+^2 \rangle} + \frac{\langle N_-(N_- - 1) \rangle}{\langle N_-^2 \rangle} - 2 \frac{\langle N_- N_+ \rangle}{\langle N_- \rangle \langle N_+ \rangle}$, where $\langle N_- \rangle$ and $\langle N_+ \rangle$ are average negative and positive charged particle multiplicity, respectively [83].

Figure 9 shows the product of $\nu(+-, dyn)$ and $\langle N_{ch} \rangle$ (average number of charged particles) as a function of $\sqrt{s_{NN}}$ [79–81]. We find that this fluctuation observable rapidly decreases with $\sqrt{s_{NN}}$ and approaches expectation from this observable for a simple QGP-like scenario [82] as we move from RHIC to LHC energies. Given that several other observables already indicate that a hot and dense medium of color charges has been formed at RHIC and LHC, this result may indicate that the observable $\nu(+-, dyn)$ is not sensitive enough to QGP physics or the process of hadronization washes out the QGP signal for this observable. It may be also noted that the models results does not incorporate the acceptance effects and does not consider any dynamic evolution of the system like for example the dilution of the signals in the hadronization process.

B. Azimuthal anisotropy

1. Energy dependence of p_T integrated v_2

Figure 10 shows the p_T integrated v_2 close to midrapidity for charged particles for collision centralities around 20-30% as a function of center of mass energy. We observe that there is an increase in magnitude of v_2 by about 30% from top RHIC energy ($\sqrt{s_{NN}} = 200$ GeV) to LHC energy ($\sqrt{s_{NN}} = 2.76$ TeV). This needs to be viewed within the context of a similar magnitude of increase in $\langle m_T \rangle$ of pions from RHIC to LHC energies. The increase of v_2 beyond beam energy of 10 AGeV is logarithmic in $\sqrt{s_{NN}}$. This is expected to be determined by the pressure gradient-driven expansion of the almond-shape fireball produced in the initial stages of a non-central heavy-ion collision [84]. While for v_2 measured at lower beam energies, the dependences observed is due to interplay of passing time of spectators and time scale of expansion of the system. A preference for an in-plane emission versus out-of-plane (“squeeze-out”) pattern of particles as a func-

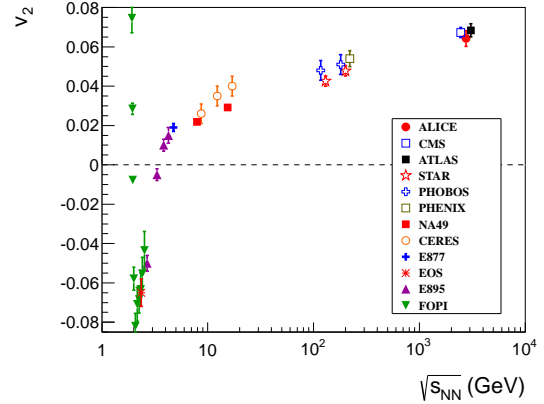


FIG. 10: (Color online) Transverse momentum integrated v_2 close to midrapidity for charged ($Z = 1$) particles for collision centralities around 20-30% as a function of center of mass energy.

tion of beam energy is observed. The experimental data used are from FOPI [85, 86], EOS, E895 [87], E877 [88], CERES [89], NA49 [90], STAR [91], PHOBOS [92], PHENIX [93], ALICE [19], ATLAS [94] and CMS [17] experiments. Charged particles are used for LHC, RHIC, CERES and E877 experiments, pion data is used from NA49 experiment, protons results are from EOS and E895 experiment and FOPI results are for all particles with $Z=1$.

2. Azimuthal anisotropy coefficients versus transverse momentum

Figure 11(top) shows the comparison of $v_2(p_T)$, $v_3(p_T)$ and $v_4(p_T)$ at RHIC (PHENIX experiment [95]) and LHC (ALICE [96]) at midrapidity for 30-40% Au+Au and Pb+Pb collisions respectively. The bottom panel of this figure shows the ratio of LHC and RHIC results to a polynomial fit to the LHC data. The $v_n(p_T)$ measurement techniques are similar at RHIC and LHC energies. One observes that at lower p_T (< 2 GeV/c) the $v_2(p_T)$ and $v_3(p_T)$ are about 10-20% smaller at RHIC compared to the corresponding LHC results. However at higher p_T the results are quite similar. The $v_4(p_T)$ seems higher at RHIC compared to LHC.

One of the most striking observations to come out from RHIC is the number of constituent quark (n_q) scaling of $v_2(p_T)$ for identified hadrons. The basis of such a scaling is the splitting of $v_2(p_T)$ between baryons and mesons at intermediate p_T (2 - 6 GeV/c). This is shown in the bottom panels of the bottom Fig. 11. Such a splitting between baryon and meson $v_2(p_T)$ is also observed at intermediate p_T at

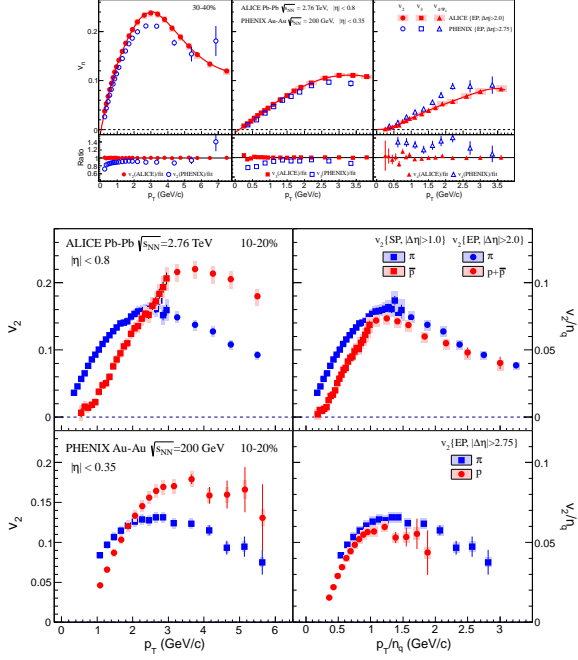


FIG. 11: (Color online) Top: Comparison of $v_n(p_T)$ at midrapidity for 30-40% collision centrality at RHIC (Au+Au collisions at $\sqrt{s_{NN}} = 200$ GeV from PHENIX experiment [95]) and at LHC (Pb+Pb collisions at $\sqrt{s_{NN}} = 2.76$ TeV from ALICE experiment [96]). The bottom panel shows the ratio of v_n at LHC and RHIC. Bottom: v_2 versus p_T and v_2/n_q versus p_T/n_q for pion and protons at midrapidity for 10-20% collision centrality from Au+Au collisions at $\sqrt{s_{NN}} = 200$ GeV (PHENIX experiment [97]) and Pb+Pb collisions at $\sqrt{s_{NN}} = 2.76$ TeV (ALICE experiment [98]).

LHC energies (seen in the top panels of the bottom Fig. 11). However the degree to which n_q scaling holds could be different at RHIC [97] and LHC [98] energies. The n_q scaling is much more closely followed at RHIC compared to LHC. It may be noted that there are several factors which could dilute such scalings, which includes energy dependence of radial flow, an admixture of higher Fock states and consideration of a realistic momentum distribution of quarks inside a hadron [99, 100]. The observation of the baryon-meson splitting is commonly interpreted as due to substantial amount of collectivity being generated in the de-confined phase. Another important feature is that at both RHIC and LHC energies a clear hydrodynamic feature of mass dependence of $v_2(p_T)$ is observed at low p_T (< 2 GeV/c).

Figure 12 shows the charged hadron $v_2(p_T)$ for 30-40% collision centrality in Au+Au collisions at $\sqrt{s_{NN}} = 200$ GeV and Pb+Pb collisions at $\sqrt{s_{NN}} = 2.76$ TeV for $|\eta| < 1$ [17]. This figure demonstrates the kinematic reach for higher energy collisions at LHC relative to RHIC. LHC data allows us to study

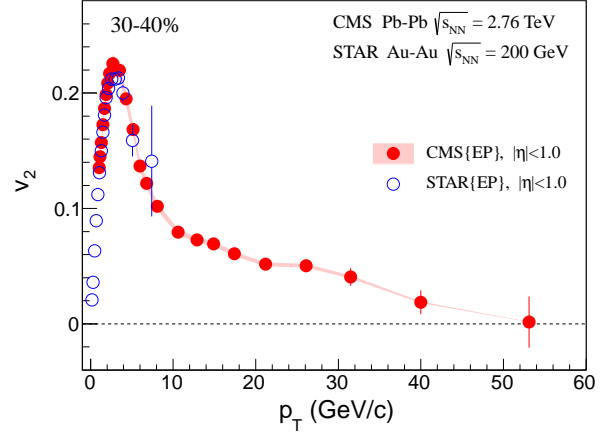


FIG. 12: (Color online) Comparison of $v_2(p_T)$ at midrapidity for 30-40% collision centrality at RHIC (Au+Au collisions at $\sqrt{s_{NN}} = 200$ GeV from STAR experiment) and at LHC (Pb+Pb collisions at $\sqrt{s_{NN}} = 2.76$ TeV from CMS experiment [17]). The shaded band about CMS data point are systematic errors and vertical lines represent statistical errors.

the $v_2(p_T)$ in the p_T range never measured before in heavy-ion collisions. The $v_2(p_T) \sim 0$ for $p_T > 40$ GeV/c suggesting that those particles must have been emitted very early in the interactions, when collective effects had not set in. These high transverse momentum data is useful to understand the effects of the initial geometry or path-length dependence of various properties associated with parton modification inside the hot QCD medium. In addition, it also provides significantly improved precision measurement of v_2 for $12 < p_T < 20$ GeV/c.

3. Flow fluctuations

Fluctuations in azimuthal anisotropy coefficient v_2 have gained quite an attention in recent times. In particular, the measurement of event-by-event v_2 fluctuations can pose new constraints on the models of the initial state of the collision and its subsequent hydrodynamic evolution. In extracting event-by-event v_2 fluctuations one needs to separate non-flow effects and so far there is no direct method to decouple v_2 fluctuations and non-flow effects in a model independent way from the experimental measurements. However, several techniques exists where the non-flow effects can be minimized, for example, flow and non-flow contributions can be possibly separated to a great extent with a detailed study of two particle correlation function in $\Delta\phi$ and its dependence on η and $\Delta\eta$. Here we discuss another technique to extract and compare the v_2 fluctuations at RHIC and LHC. We as-

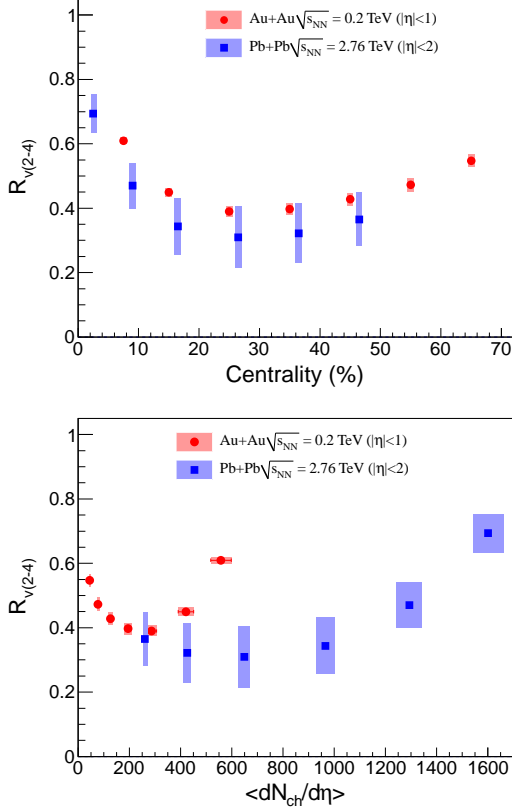


FIG. 13: (Color online) The ratio $R_{v(2-4)} = \sqrt{(v_2\{2\}^2 - v_2\{4\}^2)/(v_2\{2\}^2 + v_2\{4\}^2)}$, a measure of upper limit of v_2 fluctuations plotted as a function of collision centrality (top panel) and average number $dN_{ch}/d\eta$ (bottom panel) for RHIC (STAR experiment: Au+Au collisions at $\sqrt{s_{NN}} = 200$ GeV [101]) and LHC (ALICE: Pb+Pb collisions at $\sqrt{s_{NN}} = 2.76$ TeV [98]) at midrapidity. The bands reflect the systematic errors.

sume that the difference between $v_2\{2\}$ (two particle cumulant) and $v_2\{4\}$ (four particle cumulant) is dominated by v_2 fluctuations and non-flow effect is negligible for $v_2\{4\}$. Then the ratio $R_{v(2-4)} = \sqrt{(v_2\{2\}^2 - v_2\{4\}^2)/(v_2\{2\}^2 + v_2\{4\}^2)}$ can be considered as an upper limit for v_2 fluctuations in the data. Figure 13 shows the $R_{v(2-4)}$ as a function of collision centrality and $dN_{ch}/d\eta$ for RHIC [101] and LHC [98] energies. The centrality dependence of $R_{v(2-4)}$ at RHIC or LHC as seen in Fig. 13 could be an interplay of residual non-flow effects which increases for central collisions and multiplicity fluctuations which dominates smaller systems. It is striking to see that $R_{v(2-4)}$ when presented as a function of % cross section is similar at RHIC and LHC suggesting it reflects features associated with initial state of the collisions for example the event-by-event fluctuations in the eccentricity of the system. But when presented as a function of $dN_{ch}/d\eta$ it tends to suggest a different behaviour for central most collisions at RHIC.

C. Nuclear modification factor

Figure 14 shows the R_{AA} of various particles produced in heavy-ion collisions at RHIC and LHC. In Fig. 14(a), we observe that the shape of the R_{AA} versus p_T of charged hadrons at RHIC and LHC [20, 21] are very similar for the common p_T range of measurements. The values R_{AA} at RHIC are higher compared to those at LHC energies up to $p_T < 8$ GeV/c. The higher kinematic reach of LHC in p_T allows us to see the full p_T evolution of R_{AA} in high energy heavy-ion collisions. All these suggests the energy loss of partons in the medium formed in heavy-ion collisions at LHC energies is perhaps larger compared to those at RHIC. In Fig. 14(b), we observe that the nuclear modification factors for d+Au collisions at $\sqrt{s_{NN}} = 200$ GeV [102] and p+Pb collisions at $\sqrt{s_{NN}} = 5.02$ TeV [104] are greater than unity for the $p_T > 2$ GeV/c. The values for RHIC are slightly larger compared to those for LHC. A value greater than unity for the nuclear modification factor in $p(d)+A$ collisions are generally interpreted as due to Cronin effect [105, 106]. However several other physics effects could influence the magnitude of the nuclear modification factor in $p(d)+A$ collisions, which includes nuclear shadowing and gluon saturation effects. But the fact that the nuclear modification factor in $p(d)+A$ collisions are not below unity, experimentally strengthens the argument for formation of a hot and dense medium of color charges in A+A collisions at RHIC and LHC. In Fig. 14(c), we show the R_{AA} of particles than do not undertake strong interactions and some of them are most likely formed in the very early stages of the collisions. These particles (photon [107, 108], W^\pm [109] and Z [110] bosons) have a $R_{AA} \sim 1$, indicating that the $R_{AA} < 1$ observed for charged hadrons in A+A collisions are arising due to strong interactions in a dense medium consisting of color charges.

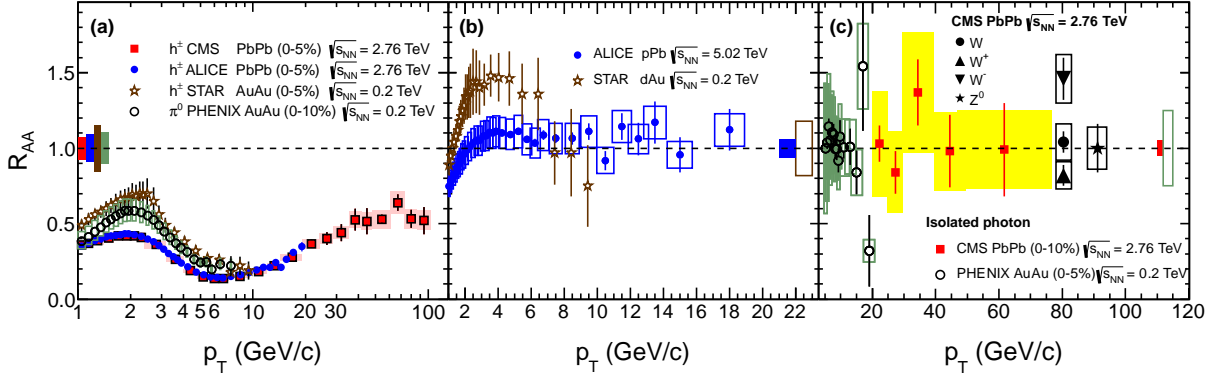


FIG. 14: (Color online) (a) Nuclear modification factor R_{AA} of charged hadrons measured by ALICE [20] and CMS [21] experiments at midrapidity for 0-5% most central Pb+Pb collisions at $\sqrt{s_{NN}} = 2.76$ TeV. For comparison shown the R_{AA} of charged hadrons at midrapidity for 0-5% most central collisions measured by STAR [102] and R_{AA} of π^0 at midrapidity for 0-10% most central collisions measured by PHENIX [103] for Au+Au collisions at $\sqrt{s_{NN}} = 200$ GeV. The boxes around the data denote p_T -dependent systematic uncertainties. The systematic uncertainties on the normalization are shown as boxes at $R_{AA} = 1$. (b) Comparison of nuclear modification factor for charged hadrons versus p_T at midrapidity for minimum bias collisions in $d+Au$ collisions at $\sqrt{s_{NN}} = 200$ GeV [102] and $p+Pb$ collisions at $\sqrt{s_{NN}} = 5.02$ TeV [104]. (c) The nuclear modification factor versus p_T for isolated photons in central nucleus-nucleus collisions at $\sqrt{s_{NN}} = 200$ GeV [107] and 2.76 TeV [108]. Also shown are the R_{AA} of W^\pm [109] and Z bosons [110] at LHC energies.

IV. COMPARISON TO MODEL CALCULATIONS

In this section, we compare some of the experimental observables discussed above with corresponding model calculations. This helps us to interpret the data at both RHIC and LHC energies. The observables chosen are the charged particle multiplicity density, ratio of kaon to pion yields as a function of beam energy, and transverse momentum dependence of v_2 and R_{AA} .

A. Charged particle multiplicity density and particle ratio

Figure 15 compares the measured charged particle pseudorapidity density at RHIC (0.2 TeV) and LHC (2.76 TeV) energies to various model calculations.

Empirical extrapolation from lower energy data (named “Busza” in the figure) [111] significantly under predicts the measurement at LHC energies. A simple power-law growth of charged-particle multiplicities near midrapidity in central Au+Au collisions seem to be followed up to RHIC energies (named as “Barshay et. al” in the figure) [112]. Perturbative QCD-inspired Monte Carlo event generators, the HIJING model without jet quenching [113], the Dual Parton Model [114] (named “DPMJET III” in the figure), or the Ultra-relativistic Quantum Molecular Dynamics model [115] (named “UrQMD”

in the figure) are consistent with the measurement. The HIJING model results without jet quenching was also consistent with the RHIC measurements. The semi-microscopic models like LEXUS are successful in explaining the observed multiplicity at RHIC (named as “Jeon et. al” in the figure) [116]. Models based on initial-state gluon density saturation have a range of predictions depending on the specifics of the implementation [117–121]. The best agreement with LHC data happens for model as described in (named as “Kharzeev1” and “Armesto” in the figure) [119, 121]. Similar are the conclusions for RHIC energy from these models. The prediction of a hybrid model based on hydrodynamics and saturation of final-state phase space of scattered partons (named as “Eskola” in the figure) [122] is slightly on higher side compared to the measurement at LHC. But such a model seems to do a reasonable job for RHIC energies [123]. Another hydrodynamic model in which multiplicity is scaled from p+p collisions over predicts the measurement (named as “Bozek” in the figure) [124]. Models incorporating scaling based on Landau hydrodynamics (named as “Sarkisyan” in the figure) [125] and based on modified PYTHIA and hadronic re-scattering (named as “Humanic” in the figure) [126] under predicts the measurement at LHC energy. At RHIC energies, models considering minijet production in ultra-relativistic heavy-ion collisions by taking semi-hard parton re-scatterings explicitly into account under predicts the multiplicities (named as “Accardi et. al in the fig-

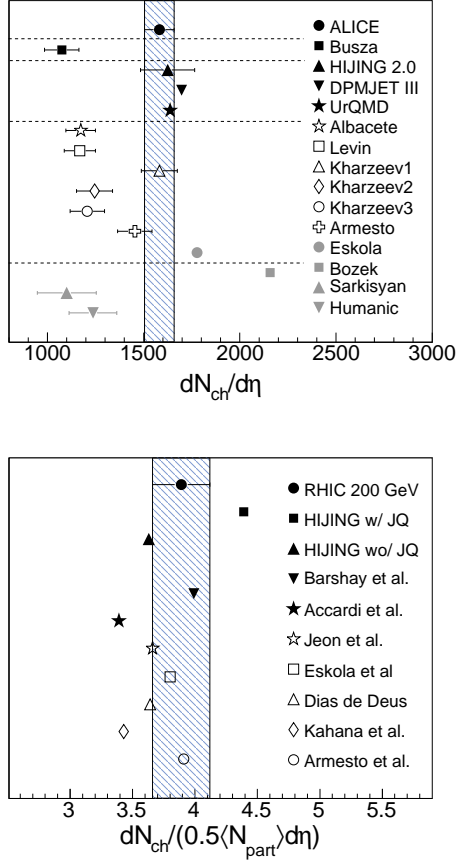


FIG. 15: (Color online) Comparison of $dN_{ch}/d\eta$ measurement at midrapidity for central heavy-ion collisions at RHIC and LHC with model predictions.

ure) [127]. It is also seen at RHIC energies that models based on string fusion [128], dual string model [129] seem to work well, whereas those based on heavy ion cascade LUCIFER model [130] under predicts the data.

Figure 16 shows the $(dN_{ch}/d\eta)/(\langle N_{part} \rangle/2)$ versus $\langle N_{part} \rangle$ for Pb+Pb collisions at $\sqrt{s_{NN}} = 2.76$ TeV [14]. Also shown are the corresponding RHIC results scaled up by a factor 2.15. Remarkable similarity is observed in the shape of the distributions at RHIC and LHC energies. Particle production based on saturation model explains the trends nicely (named as “Albacete et al” in the figure) [131]. Simple fit to the data using a power law form for the $\langle N_{part} \rangle$ also explains the measurements. In addition a functional form inspired by the detailed shape of pseudorapidity distribution of charged particle multiplicity distributions at RHIC [39] explains the centrality trends nicely.

Strangeness production in heavy-ion collisions is a classic signature for formation of QGP [132]. The particle yield ratio K/π could reflect the strangeness

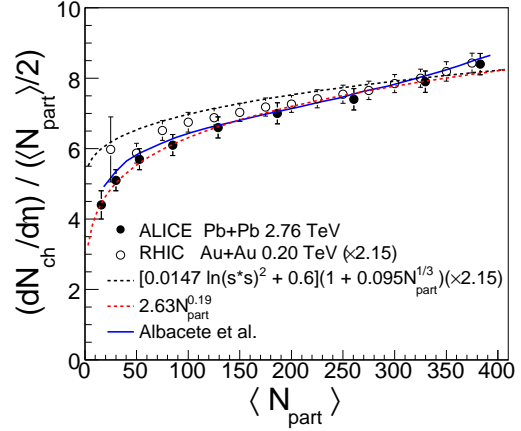


FIG. 16: (Color online) Centrality dependence of $(dN_{ch}/d\eta)/(\langle N_{part} \rangle/2)$ on $\langle N_{part} \rangle$ for Pb+Pb collisions at $\sqrt{s_{NN}} = 2.76$ TeV and Au+Au collisions at $\sqrt{s_{NN}} = 200$ GeV. The RHIC results are scaled up by a factor of 2.15. Also shown are comparisons to theoretical model calculations and some parametrization based on detail shape of $dN_{ch}/d\eta$ distributions at RHIC [39] and $\langle N_{part} \rangle$.

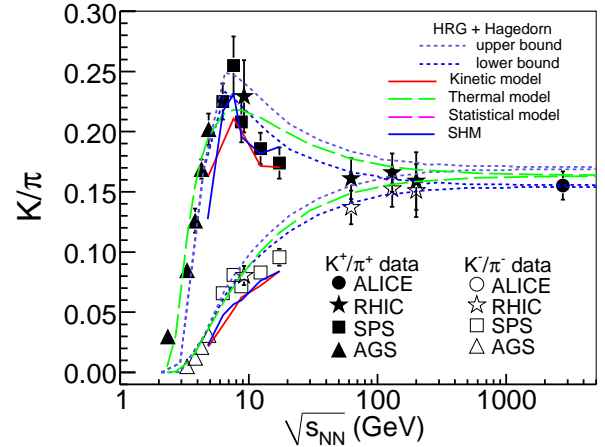


FIG. 17: (Color online) Energy dependence of K^\pm/π^\pm ratio for central collisions at midrapidity. Errors are statistical and systematic added in quadrature. Results are also compared with various theoretical model predictions [134–138].

enhancement in heavy-ion collisions with respect to the elementary collisions. Figure 17 shows the energy dependence of K^\pm/π^\pm ratio for central collisions at midrapidity. It will be interesting to see which model explains such an impressive collection of systematic data on K/π ratio. Figure 17 also shows the energy dependence of K/π ratio from various theoretical model calculations. The energy de-

pendence of K^+/π^+ ratio has been interpreted using the Statistical Model of Early Stage (SMES) [133]. The model predicts first order phase transition and the existence of mixed phase around beam energy of 7-8 GeV. The SHM or Statistical Hadronization Model [134] assumes that the strong interactions saturate the particle production matrix elements. This means that the yield of particles are controlled predominantly by the magnitude of the accessible phase space. The system is in chemical non-equilibrium for $\sqrt{s_{NN}} < 7.6$ GeV, while for higher energies, the over-saturation of chemical occupancies is observed. The Statistical Model [135] assumes that the ratio of entropy to T^3 as a function of collision energy increases for mesons and decreases for baryons. Thus, a rapid change is expected at the crossing of the two curves, as the hadronic gas undergoes a transition from a baryon-dominated to a meson-dominated gas. The transition point is characterized by $T=140$ MeV, $\mu_B=410$ MeV, and $\sqrt{s_{NN}}=8.2$ GeV. In the Thermal Model [136], the energy dependence of K^\pm/π^\pm is studied by including σ -meson, which is neglected in most of the models, and many higher mass resonances ($m > 2$ GeV/ c^2) into the resonance spectrum employed in the statistical model calculations. The hadronic non-equilibrium Kinetic model [137] assumes that the surplus of strange particles is produced in secondary reactions of hadrons generated in nuclear collisions. Then the two important aspects are the available energy density and the lifetime of the fireball. It is suggested that these two aspects combine in such a way so as to show a sharp peak for the strangeness-to-entropy or K/π ratio as a function of beam energy. In the Hadron Resonance Gas and Hagedorn model (HRG+Hagedorn) [138], all hadrons as given in PDG with masses up to 2 GeV/ c^2 are included. The unknown hadron resonances in this model are included through Hagedorn's formula for the density of states. The model assumes that the strangeness in the baryon sector decays to strange baryons and does not contribute to the kaon production. The energy dependence of K^\pm/π^\pm ratio seems to be best explained using HRG+Hagedorn model.

This systematic measurement of K/π ratio reveals two interesting information: (a) Around $\sqrt{s_{NN}} = 8$ GeV, the K^+/π^+ ratio shows a peak while the K^-/π^- ratio increases monotonically indicating the role of the maximum baryon density at freeze-out around this collision energy and (b) for $\sqrt{s_{NN}} > 100$ GeV, pair production becomes the dominant mechanism for K^\pm production, so both the ratios K^+/π^+ and K^-/π^- approach the value of 0.16. Taking into account of different masses between pions and kaons, this asymptotic value corresponding to a temperature of the order of 160 MeV.

B. Azimuthal anisotropy

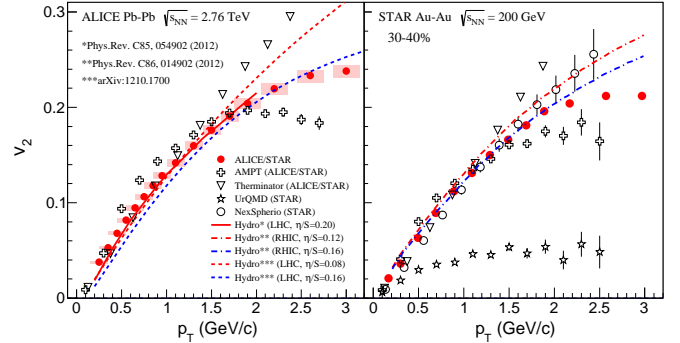


FIG. 18: (Color online) The azimuthal anisotropy parameter v_2 measured in non-central heavy-ion collisions at midrapidity for RHIC and LHC energies. For comparison, shown are the various theoretical calculations based on hydrodynamic and transport approaches (see text for details).

The azimuthal anisotropy parameter v_2 measured at RHIC and LHC provides an unique opportunity to study the transport properties of the fundamental constituents of any visible matter - a system of quarks and gluons. Further, it provides an opportunity to understand whether the underlying dynamics of the evolution of the system formed in the collisions is governed by macroscopic hydrodynamics [139–141] or by microscopic transport approach [142]. Figure 18 shows the v_2 versus p_T for 30-40% collision centrality Au+Au and Pb+Pb collisions at midrapidity for $\sqrt{s_{NN}} = 200$ GeV and 2.76 TeV, respectively. The measurements are compared to a set of model calculations based on hydrodynamic approach (including THERMINATOR [143, 144]) and another set of calculations based on transport approach. It is observed that hydrodynamic based models explain the v_2 measurements both at RHIC and LHC energies. Transport based models including partonic interactions (like AMPT [142]) also explain the v_2 measurements. However, those transport models which do not incorporate partonic interactions like UrQMD [145, 146] fail to explain the data. The model comparison also reveals that data seem to suggest a high degree of fluidity reflected by a small value of shear viscosity to entropy density ratio (η/s) < 0.2 being supported by the measurements. A more detail comparison of the model calculations with various order azimuthal anisotropy parameter v_n would in near future give us a more quantitative picture of the temperature (or energy) dependence of transport coefficients of the system formed in the heavy-ion collisions.

C. Nuclear modification factor

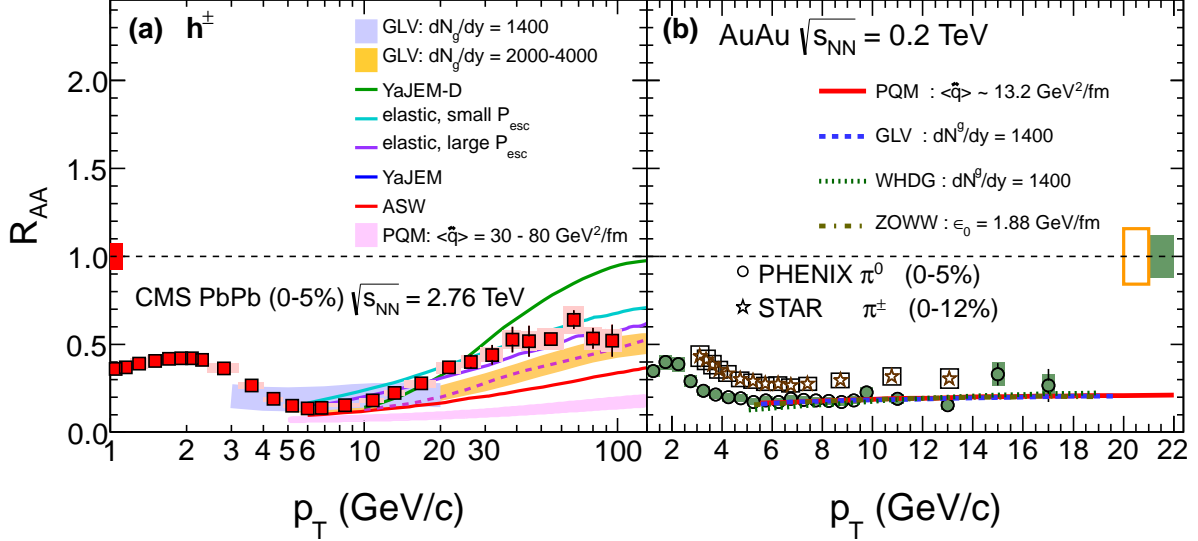


FIG. 19: (Color online) Measurements of the nuclear modification factor R_{AA} in central heavy-ion collisions at two different center-of-mass energies, as a function of p_T , for pions ($\pi^{\pm,0}$) [147, 148] and charged hadrons [20, 21], compared to several theoretical predictions (see text). The error bars on the points are the statistical uncertainties, and the boxes around the data points are the systematic uncertainties. Additional absolute normalization uncertainties of order 5% to 10% are not plotted. The bands for several of the theoretical calculations represent their uncertainties.

The nuclear modification factor (R_{AA}) is an observable used to study the structure of strongly interacting dense matter formed in heavy-ion collisions. Here we discuss the observation of $R_{AA} < 1$ at high p_T seen at RHIC and LHC by comparing to models within perturbative QCD (pQCD) based formalisms. In this picture, the high p_T hadrons are expected to originate from the fragmentation of hard partons (hard scattering scales large than QCD scales of 200 MeV). The hard partons lose energy through interactions with the hot and dense medium, which get reflected in the observed values of R_{AA} . The processes by which they could lose energy includes radiative energy loss and elastic energy loss. For a more elaborate discussion on these models we refer the reader to the review article [149].

In Fig. 19, we show a comparison between experimentally measured R_{AA} versus p_T at LHC and RHIC energies to corresponding pQCD based model calculations. All theoretical formalisms requires a microscopic model of the medium to set the input parameters for the energy loss calculation. These parameters for example are denoted as $\langle \hat{q} \rangle$, the transport coefficient of the medium or the gluon number density dN_g/dy per unit rapidity. The parameter P_{esc} on the other hand, reflects the strength of elastic energy loss put in the model calculations. Without going into deeper theoretical discussions of each model, we refer the readers to the following related publications: PQM [150], GLV [151], ASW [152], YaJEM [153], WHDG [154] and ZOWW [155]. However, for completeness and to elucidate the approach taken in the model calculations, we briefly mention as a example that two formalisms: the GLV approach named after their authors Gyulassy, Levai and Vitev and ASW approach named after the corresponding authors Armesto, Salgado and Wiedemann model, the medium as separated heavy static scattering centers with color screened potentials. Where as in some other formalism a more precise definition of the medium is considered like being composed of quark gluon quasi-particles with dispersion relations and interactions given by the hard thermal loop effective theory.

We observe that most models predict the p_T dependence of R_{AA} well for collisions both at RHIC and LHC energies. The models specially capture the generally rising behavior of R_{AA} that is observed in the data at high p_T for the LHC energies. The magnitude of the predicted slope of R_{AA} versus p_T varies between models, depending on the assumptions for the jet-quenching mechanism. The models do not seem to indicate

the need for larger values of medium density parameters in the calculation to explain the R_{AA} at RHIC and LHC for the common kinematic range. However, it seems they may require a high medium density to explain the values of R_{AA} for $p_T > 20$ GeV/ c .

V. SUMMARY

In summary, the results on multiplicity density in pseudorapidity, HBT, azimuthal anisotropy, nuclear modification factor from LHC experiments indicate that the fireball produced in the nuclear collisions is hotter, lives longer and expands to a larger size at freeze-out compared to lower energies. These results also confirm the formation of a de-confined state of quarks and gluons at RHIC energies and provide a unique kinematic access in the measurements to study in detail, the properties (such as transport coefficients) of this system of quarks and gluons.

In this review, we first showed that the first set of measurements made by the three LHC experiments with a heavy-ion program, ALICE, CMS and ATLAS, show a high degree of consistency. These measurements includes, centrality dependence of charged particle multiplicity, azimuthal anisotropy and nuclear modification factor measurements versus transverse momentum. Next we discussed the comparison of various measurements made at RHIC and LHC energies. LHC measurements of $dN_{ch}/d\eta$ clearly demonstrated the power law dependence of charged particle multiplicity on the beam energy. The LHC results also reconfirmed the observation at RHIC that particle production mechanism is not a simple superposition of several $p+p$ collisions. The $\langle m_T \rangle$, ϵ_{Bj} , freeze-out volume, decoupling time for hadrons, $\langle v_2 \rangle$ and $\langle \beta \rangle$ are larger at LHC energies compared to RHIC. This is even though the freeze-out temperatures are comparable. The net-charge fluctuations measure rapidly approach from RHIC to LHC towards a simple model based calculation for QGP state. Although the sensitivity of this observ-

able for a heavy-ion system as well as lack of proper modeling of the heavy-ion system theoretically for such an observable needs careful consideration. The v_2 fluctuations as a function of centrality fraction have a similar value at both RHIC and LHC. This reflects their sensitivity to initial state effects. Just like the $d+Au$ and direct photon R_{AA} measurements experimentally proved that the observed $R_{AA} < 1$ for charged hadrons is a final state effect at RHIC, so also the $p+Pb$, direct photon, W^\pm and Z^0 R_{AA} measurements at LHC showed that the observed $R_{AA} < 1$ is indeed due to formation of a dense medium of colored charges. All these conclusions were further validated by the comparison of several observables to corresponding model calculations in the previous section. This includes the finding that the fluid at LHC still shows a high degree of fluidity reflected by a small value of shear viscosity to entropy density ratio.

Measurements related heavy quark production [156–158], dilepton production, jet-hadron correlations [159, 160] and higher order azimuthal anisotropy [161, 162] which are now coming out of both RHIC and LHC experiments will provide a much more detail characterization of the properties of the QCD matter formed in heavy-ion collisions.

Acknowledgments

We would like to thank F. Antinori, S. Gupta, D. Keane, A. K. Mohanty, Y. P. Viyogi, and N. Xu, for reading the manuscript, helpful discussions and comments. BM is supported by the DAE-SRC project fellowship for this work. LK is supported by DOE grant DE-FG02-89ER40531 for carrying out this work.

-
- [1] B. Mohanty, New J. Phys. **13**, 065031 (2011) [arXiv:1102.2495 [nucl-ex]].
 - [2] B. Mohanty, Nucl. Phys. A **830**, 899C (2009) [arXiv:0907.4476 [nucl-ex]].
 - [3] K. Fukushima and T. Hatsuda, Rept. Prog. Phys. **74**, 014001 (2011) [arXiv:1005.4814 [hep-ph]].
 - [4] S. Gupta, X. Luo, B. Mohanty, H. G. Ritter and N. Xu, Science **332** (2011) 1525 [arXiv:1105.3934 [hep-ph]].
 - [5] A. Bazavov, T. Bhattacharya, M. Cheng, C. DeTar, H. T. Ding, S. Gottlieb, R. Gupta and P. Hegde *et al.*, Phys. Rev. D **85**, 054503 (2012) [arXiv:1111.1710 [hep-lat]].
 - [6] S. Borsanyi *et al.* [Wuppertal-Budapest Collaboration], JHEP **1009**, 073 (2010) [arXiv:1005.3508 [hep-lat]].
 - [7] I. Arsene *et al.* [BRAHMS Collaboration], Nucl. Phys. A **757**, 1 (2005) [nucl-ex/0410020].
 - [8] B. B. Back, M. D. Baker, M. Ballintijn, D. S. Barton, B. Becker, R. R. Betts, A. A. Bickley and R. Bindel *et al.*, Nucl. Phys. A **757**, 28 (2005) [nucl-ex/0410022].
 - [9] J. Adams *et al.* [STAR Collaboration], Nucl. Phys. A **757**, 102 (2005) [nucl-ex/0501009].
 - [10] K. Adcox *et al.* [PHENIX Collaboration], Nucl. Phys. A **757**, 184 (2005) [nucl-ex/0410003].
 - [11] M. Gyulassy and L. McLerran, Nucl. Phys. A **750**, 30 (2005) [nucl-th/0405013].

- [12] B. Mohanty [STAR Collaboration], J. Phys. G **38**, 124023 (2011) [arXiv:1106.5902 [nucl-ex]].
- [13] M. L. Miller, K. Reygers, S. J. Sanders and P. Steinberg, Ann. Rev. Nucl. Part. Sci. **57**, 205 (2007) [nucl-ex/0701025].
- [14] K. Aamodt *et al.* [ALICE Collaboration], Phys. Rev. Lett. **106**, 032301 (2011) [arXiv:1012.1657 [nucl-ex]].
- [15] S. Chatrchyan *et al.* [CMS Collaboration], JHEP **1108**, 141 (2011) [arXiv:1107.4800 [nucl-ex]].
- [16] G. Aad *et al.* [ATLAS Collaboration], Phys. Lett. B **710**, 363 (2012) [arXiv:1108.6027 [hep-ex]].
- [17] S. Chatrchyan *et al.* [CMS Collaboration], Phys. Rev. Lett. **109**, 022301 (2012) [arXiv:1204.1850 [nucl-ex]].
- [18] G. Aad *et al.* [ATLAS Collaboration], Phys. Lett. B **707**, 330 (2012) [arXiv:1108.6018 [hep-ex]].
- [19] K. Aamodt *et al.* [ALICE Collaboration], Phys. Rev. Lett. **105**, 252302 (2010) [arXiv:1011.3914 [nucl-ex]].
- [20] K. Aamodt *et al.* [ALICE Collaboration], Phys. Lett. B **696**, 30 (2011) [arXiv:1012.1004 [nucl-ex]].
- [21] S. Chatrchyan *et al.* [CMS Collaboration], Eur. Phys. J. C **72**, 1945 (2012) [arXiv:1202.2554 [nucl-ex]].
- [22] B. B. Back *et al.* [PHOBOS Collaboration], Phys. Rev. Lett. **93**, 082301 (2004) [nucl-ex/0311009].
- [23] M. C. Abreu *et al.* [NA50 Collaboration], Phys. Lett. B **530**, 33 (2002).
- [24] C. Adler *et al.* [STAR Collaboration], Phys. Rev. Lett. **87**, 112303 (2001) [nucl-ex/0106004].
- [25] I. G. Bearden *et al.* [BRAHMS Collaboration], Phys. Lett. B **523**, 227 (2001) [nucl-ex/0108016].
- [26] I. G. Bearden *et al.* [BRAHMS Collaboration], Phys. Rev. Lett. **88**, 202301 (2002) [nucl-ex/0112001].
- [27] K. Adcox *et al.* [PHENIX Collaboration], Phys. Rev. Lett. **86**, 3500 (2001) [nucl-ex/0012008].
- [28] B. B. Back *et al.* [PHOBOS Collaboration], Phys. Rev. Lett. **85**, 3100 (2000) [hep-ex/0007036].
- [29] B. B. Back, M. D. Baker, D. S. Barton, R. R. Betts, M. Ballintijn, A. A. Bickley, R. Bindel and A. Budzanowski *et al.*, Phys. Rev. Lett. **91**, 052303 (2003) [nucl-ex/0210015].
- [30] K. Aamodt *et al.* [ALICE Collaboration], Phys. Rev. Lett. **105**, 252301 (2010) [arXiv:1011.3916 [nucl-ex]].
- [31] C. Albajar *et al.* [UA1 Collaboration], Nucl. Phys. B **335**, 261 (1990).
- [32] K. Alpgard *et al.* [UA5 Collaboration], Phys. Lett. B **121**, 209 (1983); G. Alner *et al.* [UA5 Collaboration], Z. Phys. C **33**, 1 (1986);
- [33] B. I. Abelev *et al.* [STAR Collaboration], Phys. Rev. C **79**, 034909 (2009) [arXiv:0808.2041 [nucl-ex]].
- [34] F. Abe *et al.* [CDF Collaboration], Phys. Rev. D **41**, 2330 (1990).
- [35] K. Aamodt *et al.* [ALICE Collaboration], Eur. Phys. J. C **68**, 345 (2010) [arXiv:1004.3514 [hep-ex]].
- [36] V. Khachatryan *et al.* [CMS Collaboration], JHEP **1002**, 041 (2010) [arXiv:1002.0621 [hep-ex]].
- [37] W. Thome *et al.*, Nucl. Phys. B **129**, 1 (1986).
- [38] K. Aamodt *et al.* [ALICE Collaboration], Eur. Phys. J. C **68**, 89 (2010) [arXiv:1004.3034 [hep-ex]].
- [39] B. Alver *et al.* [PHOBOS Collaboration], Phys. Rev. C **83**, 024913 (2011) [arXiv:1011.1940 [nucl-ex]].
- [40] B. Abelev *et al.* [ALICE Collaboration], Phys. Rev. Lett. **110**, 032301 (2013) [Phys. Rev. Lett. **110**, 032301 (2013)] [arXiv:1210.3615 [nucl-ex]].
- [41] T. Alber *et al.* [NA35 Collaboration], Eur. Phys. J. C **2**, 643 (1998) [hep-ex/9711001].
- [42] L. Ahle *et al.* [E866 and E917 Collaborations], Phys. Lett. B **476**, 1 (2000) [nucl-ex/9910008].
- [43] J. Barrette *et al.* [E877 Collaboration], Phys. Rev. C **62**, 024901 (2000) [nucl-ex/9910004].
- [44] S. V. Afanasiev *et al.* [NA49 Collaboration], Phys. Rev. C **66**, 054902 (2002) [nucl-ex/0205002].
- [45] C. Alt *et al.* [NA49 Collaboration], Phys. Rev. C **77**, 024903 (2008) [arXiv:0710.0118 [nucl-ex]].
- [46] B. I. Abelev *et al.* [STAR Collaboration], Phys. Rev. C **81**, 024911 (2010) [arXiv:0909.4131 [nucl-ex]].
- [47] B. Abelev *et al.* [ALICE Collaboration], Phys. Rev. Lett. **109**, 252301 (2012) [arXiv:1208.1974 [hep-ex]].
- [48] J. D. Bjorken, Phys. Rev. D **27**, 140 (1983).
- [49] C. Loizides, J. Phys. G **38**, 124040 (2011) [arXiv:1106.6324 [nucl-ex]].
- [50] S. Chatrchyan *et al.* [CMS Collaboration], Phys. Rev. Lett. **109**, 152303 (2012) [arXiv:1205.2488 [nucl-ex]].
- [51] J. T. Mitchell [PHENIX Collaboration], arXiv:1211.6139 [nucl-ex].
- [52] S. S. Adler *et al.* [PHENIX Collaboration], Phys. Rev. C **71**, 034908 (2005) [Erratum-ibid. C **71**, 049901 (2005)] [nucl-ex/0409015].
- [53] K. Adcox *et al.* [PHENIX Collaboration], Phys. Rev. Lett. **87**, 052301 (2001) [nucl-ex/0104015].
- [54] M. M. Aggarwal *et al.* [WA98 Collaboration], Eur. Phys. J. C **18**, 651 (2001) [nucl-ex/0008004].
- [55] B. Mohanty, J. -eAlam, S. Sarkar, T. K. Nayak, B. KNandi and , Phys. Rev. C **68**, 021901 (2003) [nucl-th/0304023].
- [56] L. Van Hove, Phys. Lett. B **118**, 138 (1982).
- [57] M. A. Lisa *et al.* [E895 Collaboration], Phys. Rev. Lett. **84**, 2798 (2000).
- [58] C. Alt *et al.* [NA49 Collaboration], Phys. Rev. C **77**, 064908 (2008) [arXiv:0709.4507 [nucl-ex]].
- [59] D. Adamova *et al.* [CERES Collaboration], Nucl. Phys. A **714**, 124 (2003) [nucl-ex/0207005].
- [60] B. I. Abelev *et al.* [STAR Collaboration], Phys. Rev. C **80**, 024905 (2009) [arXiv:0903.1296 [nucl-ex]].
- [61] B. B. Back *et al.* [PHOBOS Collaboration], Phys. Rev. C **73**, 031901 (2006) [nucl-ex/0409001].
- [62] K. Aamodt *et al.* [ALICE Collaboration], Phys. Lett. B **696**, 328 (2011) [arXiv:1012.4035 [nucl-ex]].
- [63] G. F. Bertsch, Nucl. Phys. A **498**, 173C (1989).
- [64] S. Pratt, Phys. Rev. D **33**, 1314 (1986).
- [65] W. Reisdorf *et al.* [FOPI Collaboration], Nucl. Phys. A **612**, 493 (1997) [nucl-ex/9610009].
- [66] M. A. Lisa *et al.* [EOS Collaboration], Phys. Rev.

- Lett. **75**, 2662 (1995) [nucl-ex/9502001].
- [67] C. Muntz [E802 Collaboration], nucl-ex/9806002.
- [68] H. Appelshauser *et al.* [NA49 Collaboration], Eur. Phys. J. C **2**, 661 (1998) [hep-ex/9711024].
- [69] A. Andronic, P. Braun-Munzinger, and J. Stachel, Nucl. Phys. A **772**, 167 (2006) [nucl-th/0511071].
- [70] A. Andronic, P. Braun-Munzinger, and J. Stachel, Phys. Lett. B **673**, 142 (2009) [Erratum-ibid. B **678**, 516 (2009)] [arXiv:0812.1186 [nucl-th]].
- [71] J. Cleymans, H. Oeschler, K. Redlich and , J. Phys. G **25**, 281 (1999) [nucl-th/9809031].
- [72] J. Cleymans, D. Elliott, A. Keranen, E. Suhoenen and , Phys. Rev. C **57**, 3319 (1998) [nucl-th/9711066].
- [73] P. Braun-Munzinger, J. Stachel, J. P. Wessels, N. Xu and , Phys. Lett. B **344**, 43 (1995) [nucl-th/9410026].
- [74] P. Braun-Munzinger, I. Heppe, J. Stachel and , Phys. Lett. B **465**, 15 (1999) [nucl-th/9903010].
- [75] F. Becattini, G. Pettini and , Phys. Rev. C **67**, 015205 (2003) [hep-ph/0204340].
- [76] F. Becattini, J. Cleymans, A. Keranen, ESuhonen, K. Redlich and , Phys. Rev. C **64**, 024901 (2001) [hep-ph/0002267].
- [77] L. Milano [for the ALICE Collaboration], arXiv:1302.6624 [hep-ex].
- [78] J. Steinheimer, J. Aichelin, M. Bleicher and , Phys. Rev. Lett. **110**, 042501 (2013) [arXiv:1203.5302 [nucl-th]].
- [79] H. Sako *et al.* [CERES/NA45 Collaboration], J. Phys. G **30**, S1371 (2004) [nucl-ex/0403037].
- [80] B. I. Abelev *et al.* [STAR Collaboration], Phys. Rev. C **79**, 024906 (2009) [arXiv:0807.3269 [nucl-ex]].
- [81] B. Abelev *et al.* [ALICE Collaboration], arXiv:1207.6068 [nucl-ex].
- [82] S. Jeon, V. Koch and , Phys. Rev. Lett. **85**, 2076 (2000) [hep-ph/0003168].
- [83] C. Pruneau, S. Gavin, S. Voloshin and , Phys. Rev. C **66**, 044904 (2002) [nucl-ex/0204011].
- [84] J. -Y. Ollitrault, Phys. Rev. D **46**, 229 (1992).
- [85] A. Andronic *et al.* [FOPI Collaboration], Phys. Lett. B **612**, 173 (2005) [nucl-ex/0411024].
- [86] N. Bastid *et al.* [FOPI Collaboration], Phys. Rev. C **72**, 011901 (2005) [nucl-ex/0504002].
- [87] P. Braun-Munzinger, J. Stachel and , Nucl. Phys. A **638**, 3 (1998) [nucl-ex/9803015].
- [88] C. Pinkenburg *et al.* [E895 Collaboration], Phys. Rev. Lett. **83**, 1295 (1999) [nucl-ex/9903010].
- [89] D. Adamova *et al.* [CERES Collaboration], Nucl. Phys. A **698**, 253 (2002).
- [90] C. Alt *et al.* [NA49 Collaboration], Phys. Rev. C **68**, 034903 (2003) [nucl-ex/0303001].
- [91] J. Adams *et al.* [STAR Collaboration], Phys. Rev. C **72**, 014904 (2005) [nucl-ex/0409033].
- [92] B. B. Back *et al.* [PHOBOS Collaboration], Phys. Rev. Lett. **94**, 122303 (2005) [nucl-ex/0406021].
- [93] S. Afanasiev *et al.* [PHENIX Collaboration], Phys. Rev. C **80**, 024909 (2009) [arXiv:0905.1070 [nucl-ex]].
- [94] [ATLAS Collaboration], ATLAS-CONF-2012-117.
- [95] A. Adare *et al.* [PHENIX Collaboration], Phys. Rev. Lett. **107**, 252301 (2011) [arXiv:1105.3928 [nucl-ex]].
- [96] K. Aamodt *et al.* [ALICE Collaboration], Phys. Rev. Lett. **107**, 032301 (2011) [arXiv:1105.3865 [nucl-ex]].
- [97] A. Adare *et al.* [PHENIX Collaboration], Phys. Rev. C **85**, 064914 (2012) [arXiv:1203.2644 [nucl-ex]].
- [98] B. Abelev *et al.* [ALICE Collaboration], arXiv:1205.5761 [nucl-ex].
- [99] B. Muller, R. J. Fries and S. A. Bass, Phys. Lett. B **618**, 77 (2005) [nucl-th/0503003].
- [100] V. Greco and C. M. Ko, nucl-th/0505061.
- [101] G. Agakishiev *et al.* [STAR Collaboration], Phys. Rev. C **86**, 014904 (2012) [arXiv:1111.5637 [nucl-ex]].
- [102] J. Adams *et al.* [STAR Collaboration], Phys. Rev. Lett. **91**, 072304 (2003) [nucl-ex/0306024].
- [103] S. S. Adler *et al.* [PHENIX Collaboration], Phys. Rev. C **76**, 034904 (2007) [nucl-ex/0611007].
- [104] B. Abelev *et al.* [ALICE Collaboration], arXiv:1210.4520 [nucl-ex].
- [105] D. Antreasyan, J. W. Cronin, H. J. Frisch, M. J. Shochet, L. Kluberg, P. A. Piroue and R. L. Sumner, Phys. Rev. Lett. **38**, 115 (1977).
- [106] D. Antreasyan, J. W. Cronin, H. J. Frisch, M. J. Shochet, L. Kluberg, P. A. Piroue and R. L. Sumner, Phys. Rev. Lett. **38**, 112 (1977).
- [107] S. S. Adler *et al.* [PHENIX Collaboration], Phys. Rev. Lett. **94**, 232301 (2005) [nucl-ex/0503003].
- [108] S. Chatrchyan *et al.* [CMS Collaboration], Phys. Lett. B **710**, 256 (2012) [arXiv:1201.3093 [nucl-ex]].
- [109] S. Chatrchyan *et al.* [CMS Collaboration], Phys. Lett. B **715**, 66 (2012) [arXiv:1205.6334 [nucl-ex]].
- [110] S. Chatrchyan *et al.* [CMS Collaboration], Phys. Rev. Lett. **106**, 212301 (2011) [arXiv:1102.5435 [nucl-ex]].
- [111] W. Busza, J. Phys. G **35**, 044040 (2008) [arXiv:0710.2293 [nucl-ex]].
- [112] S. Barshay, G. Kreyerhoff and , Nucl. Phys. A **697**, 563 (2002) [Erratum-ibid. A **703**, 891 (2002)] [hep-ph/0104303].
- [113] W. -T. Deng, X. -N. Wang, R. Xu and , Phys. Rev. C **83**, 014915 (2011) [arXiv:1008.1841 [hep-ph]].
- [114] F. W. Bopp, R. Engel, J. Ranft, S. Roesler and , arXiv:0706.3875 [hep-ph].
- [115] M. Mitrovski, T. Schuster, G. Graf, H. Petersen, M. Bleicher and , Phys. Rev. C **79**, 044901 (2009) [arXiv:0812.2041 [hep-ph]].
- [116] S. Jeon, J. I. Kapusta and , Phys. Rev. C **63**, 011901 (2001) [nucl-th/0009032].
- [117] J. LAlbacete, J. Phys. Conf. Ser. **270**, 012052 (2011) [arXiv:1010.6027 [hep-ph]].
- [118] E. Levin, A. H. Rezaeian and , Phys. Rev. D **82**, 054003 (2010) [arXiv:1007.2430 [hep-ph]].
- [119] D. Kharzeev, E. Levin, M. Nardi and , Nucl. Phys. A **747**, 609 (2005) [hep-ph/0408050].
- [120] D. Kharzeev, E. Levin, M. Nardi and , arXiv:0707.0811 [hep-ph].
- [121] N. Armesto, C. A. Salgado, U. A. Wiedemann and , Phys. Rev. Lett. **94**, 022002 (2005) [hep-ph/0407018].

- [122] K. J. Eskola, P. V. Ruuskanen, S. S. Rasanen, K. Tuominen and , Nucl. Phys. A **696**, 715 (2001) [hep-ph/0104010].
- [123] K. J. Eskola, K. Kajantie, K. Tuominen and , Nucl. Phys. A **700**, 509 (2002) [hep-ph/0106330].
- [124] P. Bozek, M. Chojnacki, W. Florkowski, B. Tomasik and , Phys. Lett. B **694**, 238 (2010) [arXiv:1007.2294 [nucl-th]].
- [125] E. K. G. Sarkisyan, A. S. Sakharov and , Eur. Phys. J. C **70**, 533 (2010) [arXiv:1004.4390 [hep-ph]].
- [126] T. J. Humanic, arXiv:1011.0378 [nucl-th].
- [127] A. Accardi, hep-ph/0104060.
- [128] N. Armesto, C. Pajares, D. Sousa and , Phys. Lett. B **527**, 92 (2002) [hep-ph/0104269].
- [129] J. Dias de Deus, R. Ugoccioni and , Phys. Lett. B **491**, 253 (2000) [hep-ph/0008086].
- [130] D. E. Kahana, S. H. Kahana and , Phys. Rev. C **63**, 031901 (2001).
- [131] J. L. ALbacete, A. Dumitru and , arXiv:1011.5161 [hep-ph].
- [132] P. Koch, B. Muller and J. Rafelski, Phys. Rept. **142**, 167 (1986).
- [133] M. Gaździcki, M. I. Gorenstein, Acta Phys. Pol. B. **30**, 2705 (1999).
- [134] I. Kuznetsova *et al.* J. Phys. G **35**, 044011 (2008).
- [135] J. Cleymans *et al.* Eur. Phys. J. A **29**, 119 (2006).
- [136] A. Andronic *et al.* Phys. Lett. B **673**, 142 (2009).
- [137] B. Tomasik *et al.* Eur. Phys. J. C **49**, 115 (2007).
- [138] S. Chatterjee *et al.* Phys. Rev. C **81**, 044907 (2010).
- [139] C. Shen and U. Heinz, Phys. Rev. C **85**, 054902 (2012) [Erratum-ibid. C **86**, 049903 (2012)] [arXiv:1202.6620 [nucl-th]].
- [140] V. Roy, A. K. Chaudhuri and B. Mohanty, Phys. Rev. C **86**, 014902 (2012) [arXiv:1204.2347 [nucl-th]].
- [141] V. Roy, B. Mohanty and A. K. Chaudhuri, arXiv:1210.1700 [nucl-th].
- [142] J. Xu and C. M. Ko, Phys. Rev. C **83**, 034904 (2011) [arXiv:1101.2231 [nucl-th]].
- [143] M. Chojnacki, A. Kisiel, W. Florkowski and W. Broniowski, Comput. Phys. Commun. **183**, 746 (2012) [arXiv:1102.0273 [nucl-th]].
- [144] A. Kisiel, T. Taluc, W. Broniowski and W. Florkowski, Comput. Phys. Commun. **174**, 669 (2006) [nucl-th/0504047].
- [145] S. A. Bass, M. Belkacem, M. Bleicher, M. Brandstetter, L. Bravina, C. Ernst, L. Gerland and M. Hofmann *et al.*, Prog. Part. Nucl. Phys. **41**, 255 (1998) [Prog. Part. Nucl. Phys. **41**, 225 (1998)] [nucl-th/9803035].
- [146] M. Bleicher, E. Zabrodin, C. Spieles, S. A. Bass, C. Ernst, S. Soff, L. Bravina and M. Belkacem *et al.*, J. Phys. G **25**, 1859 (1999) [hep-ph/9909407].
- [147] A. Adare *et al.* [PHENIX Collaboration], Phys. Rev. C **77**, 064907 (2008) [arXiv:0801.1665 [nucl-ex]].
- [148] B. I. Abelev *et al.* [STAR Collaboration], Phys. Lett. B **655**, 104 (2007) [nucl-ex/0703040].
- [149] A. Majumder and M. Van Leeuwen, Prog. Part. Nucl. Phys. A **66**, 41 (2011) [arXiv:1002.2206 [hep-ph]].
- [150] A. Dainese, C. Loizides and G. Paic, Eur. Phys. J. C **38**, 461 (2005) [hep-ph/0406201].
- [151] I. Vitev and M. Gyulassy, Phys. Rev. Lett. **89**, 252301 (2002) [hep-ph/0209161].
- [152] N. Armesto, A. Dainese, C. A. Salgado and U. A. Wiedemann, Phys. Rev. D **71**, 054027 (2005) [hep-ph/0501225].
- [153] T. Renk, H. Holopainen, R. Paatelainen and K. J. Eskola, Phys. Rev. C **84**, 014906 (2011) [arXiv:1103.5308 [hep-ph]].
- [154] S. Wicks, W. Horowitz, M. Djordjevic and M. Gyulassy, Nucl. Phys. A **784**, 426 (2007) [nucl-th/0512076].
- [155] H. Zhang, J. F. Owens, E. Wang and X. - N. Wang, Phys. Rev. Lett. **98**, 212301 (2007) [nucl-th/0701045].
- [156] S. Chatrchyan *et al.* [CMS Collaboration], JHEP **1205**, 063 (2012) [arXiv:1201.5069 [nucl-ex]].
- [157] E. Abbas *et al.* [ALICE Collaboration], arXiv:1303.5880 [nucl-ex].
- [158] L. Adamczyk *et al.* [STAR Collaboration], arXiv:1212.3304 [nucl-ex].
- [159] L. Adamczyk *et al.* [STAR Collaboration], arXiv:1302.6184 [nucl-ex].
- [160] S. Chatrchyan *et al.* [CMS Collaboration], Phys. Lett. B **718**, 795 (2013) [arXiv:1210.5482 [nucl-ex]].
- [161] L. Adamczyk, *et al.* [STAR Collaboration], arXiv:1301.2187 [nucl-ex].
- [162] G. Aad *et al.* [ATLAS Collaboration], arXiv:1303.2084 [hep-ex].